

# Three-Dimensional Engineered Bone from Bone Marrow Stromal Cells and Their Autogenous Extracellular Matrix

Fatima N. Syed-Picard, M.S.,<sup>1</sup> Lisa M. Larkin, Ph.D.,<sup>2,3</sup> Charles M. Shaw, B.S.,<sup>4</sup> and Ellen M. Arruda, Ph.D.<sup>4,5</sup>

Most bone tissue–engineering research uses porous three-dimensional (3D) scaffolds for cell seeding. In this work, scaffold-less 3D bone-like tissues were engineered from rat bone marrow stromal cells (BMSCs) and their autogenous extracellular matrix (ECM). The BMSCs were cultured on a 2D substrate in medium that induced osteogenic differentiation. After reaching confluence and producing a sufficient amount of their own ECM, the cells contracted their tissue monolayer around two constraint points, forming scaffold-less cylindrical engineered bone-like constructs (EBCs). The EBCs exhibited alizarin red staining for mineralization and alkaline phosphatase activity and contained type I collagen. The EBCs developed a periosteum characterized by fibroblasts and unmineralized collagen on the periphery of the construct. Tensile tests revealed that the EBCs in culture had a tangent modulus of  $7.5 \pm 0.5$  MPa at 7 days post-3D construct formation and  $29 \pm 9$  MPa at 6 weeks after construct formation. Implantation of the EBCs into rats 7 days after construct formation resulted in further bone development and vascularization. Tissue explants collected at 4 weeks contained all three cell types found in native bone: osteoblasts, osteocytes, and osteoclasts. The resulting engineered tissues are the first 3D bone tissues developed without the use of exogenous scaffolding.

## Introduction

APPROXIMATELY ONE MILLION surgeries are performed each year in the United States that require bone grafts to replace tissue damaged by disease or extensive trauma.<sup>1</sup> Several limitations are associated with grafting, such as graft availability, donor site morbidity, and immune rejection. Because of these complications, strategies are being developed to engineer bone tissue *in vitro* for bone replacement.

Current approaches to engineer bone involve the design of a three-dimensional (3D) scaffold that promotes the differentiation and proliferation of osteogenic cells and the deposition and mineralization of an osteogenic extracellular matrix (ECM). The scaffold design rubrics also include the ability to withstand physiological loads *in vivo* and eventual incorporation into the native tissue or degradation during the course of tissue development.<sup>2</sup> Polymers such as poly(lactic-co-glycolic acid), poly(propylene fumarates), and poly(caprolactones) provide a matrix that promotes cell adhesion and migration, allow for the deposition and mineralization of osteogenic ECM *in vitro*, and have predictable degradation rates but lack the mechanical properties needed

to withstand the loads placed on natural bone *in vivo*.<sup>3–5</sup> Hydroxyapatite and  $\beta$ -tricalcium phosphates are ceramics used for bone scaffolding that also promote cell adhesion and proliferation and when implanted have shown positive results with regard to bone regeneration *in vivo*. However, the brittle nature of ceramics inhibits their use in healing large defects.<sup>2,6</sup> Polymer–ceramic composite scaffolds such as calcium phosphate salts embedded in poly(caprolactones) have been designed to mitigate the problems with using each material alone, but a significant percentage of cells fails to attach to the composite scaffold because of limited surface-to-volume ratio.<sup>7,8</sup> Single-layer cell sheets grown from bone marrow stromal cells (BMSCs) and wrapped around composite scaffolds have recently been shown to form constructs that resemble bone *in vitro* and *in vivo*.<sup>8</sup> However, this method still involves the use of an exogenous scaffolding that must incorporate into native tissue.

BMSCs are multipotent cells that can differentiate *in vitro* in response to chemical signals and generate and mineralize their own autogenous ECM. BMSCs can be easily isolated from autologous sources and therefore serve as an attractive candidate for tissue engineering.<sup>9–12</sup> Because a specific bone

<sup>1</sup>Department of Materials Science and Engineering, University of Michigan, Ann Arbor, Michigan.

<sup>2</sup>Department of Molecular and Integrative Physiology, University of Michigan, Ann Arbor, Michigan.

<sup>3</sup>Department of Biomedical Engineering, University of Michigan, Ann Arbor, Michigan.

<sup>4</sup>Program in Macromolecular Science and Engineering, University of Michigan, Ann Arbor, Michigan.

<sup>5</sup>Department of Mechanical Engineering, University of Michigan, Ann Arbor, Michigan.

marker does not exist, an engineered tissue is characterized as being bone according to a number of criteria. The presence of alkaline phosphatase (ALP), an enzyme that cleaves phosphate ions from organic molecules, is a precursor to mineralization of bone and thus an early sign of bone formation.<sup>13</sup> Bone is composed predominantly of type I collagen mineralized with hydroxyapatite crystals and contains osteocalcin, so the presence of these molecules further substantiates differentiation of BMSCs toward bone. The absence of type II collagen, the predominant protein of cartilage, is often used to exclude differentiation to cartilage. The structural properties of bone, including cells with an osteogenic morphology and nucleation and growth of mineralized structures through matrix vesicles or intrafibrillar mineralization, can be monitored using light and electron microscopy.<sup>14</sup> The periosteum of bone is fibrous tissue found on the bone surface that contains fibroblasts, osteoprogenitor cells, and unmineralized type I collagen. Osteoprogenitor cells differentiate into osteoblasts during bone growth and remodeling.<sup>15</sup> The periosteum can be identified through microscopy because of the elongated shape of fibroblasts and osteoprogenitor cells, versus the round presentation of osteoblasts. The presence of rows of osteoblasts between the fibrous periosteum and the mineralized bone core is an indication of a functioning periosteum because the osteoprogenitor cells are actively differentiating to osteoblasts.

In this study, we developed a method to engineer 3D bone-like tissue structures solely from BMSCs and their autogenous ECM using an approach similar to one we previously developed for tissue engineering of soft tissues and their interfaces.<sup>16-18</sup> Our method bypasses the many design challenges and limitations associated with the engineering of composite bone constructs with exogenous scaffolding. The successful fabrication of engineered bone-like structures was confirmed using histological and immunofluorescent markers for ALP activity, type I collagen, osteocalcin, and absence of type II collagen. The engineered tissues were further analyzed structurally using transmission electron microscopy (TEM) and functionally with tensile tests. Our autogenous matrix engineered bone-like constructs were ectopically implanted *in vivo* to investigate the effects of an *in vivo* environment on the growth and development of the engineered tissue.

## Methods

### *BMSC isolation and expansion*

All animal care and animal surgeries were in accordance with The Guide for Care and Use of Laboratory Animals (Public Health Service, 1996, National Institutes of Health Publication No. 85-23); the University of Michigan's Committee for the Use and Care of Animals approved by the experimental protocol. Under aseptic conditions, bone marrow was collected from the femur and tibia of female Fisher 344 rats. Briefly, the soft tissues of the leg were removed from the femur and tibia, both ends of the bones were detached, and the marrow flushed out using a syringe with a 25-gauge needle filled with Dulbecco's modified Eagle medium (DMEM; Gibco, Rockville, MD). The marrow was vortexed and then centrifuged at 480 g for 5 min using a Thermo Forma General Purpose Centrifuge (Waltham, MA). The pellet was resuspended in 10 mL of growth medium (M1) consisting of DMEM with 20 volume % fetal bovine serum (Gibco), 6 ng/mL basic fibroblast

growth factor (bFGF; Peprotech, Rocky Hill, NJ),  $10^{-8}$  M dexamethasone (dex; Sigma-Aldrich, St. Louis, MO), and 1% antibiotic-antimycotic (Gibco), and plated into 100-mm-diameter tissue culture dishes. The dishes were kept in an incubator at 37°C, 95% humidity, and 5% carbon dioxide. After 48 h, the non-adherent cells were removed by replacing the M1. The adherent BMSCs were cultured to 80% confluence, at which time cells were enzymatically removed from the plate using a 0.25% trypsin-ethylenediaminetetraacetic acid solution (Gibco) and passaged. Cells were plated onto construct dishes during the third to fifth passages.

### *Construct dish preparation*

Tissue culture plastic dishes, 35 mm in diameter (BD Biosciences, San Jose, CA), were filled with 1.5 mL SYLGARD (type 184 silicone elastomer; Dow Chemical, Midland, MI). The polymer was allowed to cure for 3 weeks before use. The SYLGARD was coated with  $3 \mu\text{g}/\text{cm}^2$  natural mouse laminin (Invitrogen, Carlsbad, CA) by filling dishes with 3 mL of a 9.6 mg/mL laminin solution in Dulbecco's phosphate buffered saline (DPBS; Gibco). The laminin solution was evaporated overnight in a biosafety cabinet. Dishes were rinsed once with DPBS and then filled with 1 mL of DMEM containing 20% fetal bovine serum and 1% antibiotic-antimycotic. The dishes were then sterilized via exposure to ultraviolet radiation (wavelength, 253.7 nm; bulb G30T8) in a biological safety cabinet for 60 min, then kept in an incubator for 5 to 8 days. After the incubation, the medium was aspirated from the dish, and BMSCs were seeded onto each dish in 2 mL of M1 supplemented with 0.13 mg/mL of L-ascorbic acid-2-phosphate (asc-2-phos; Sigma-Aldrich) and 0.05 mg/mL of L-proline (Sigma-Aldrich). There were 30 dishes in total, with an initial cell density of 200,000 BMSCs/dish. The cells were fed M1 supplemented with asc-2-phos and proline every 2 days until confluence was reached. Once the cells reached confluence, two minuten pins, 0.2 mm in diameter and 1 cm long (Fine Science Tools, San Francisco, CA), were pinned onto the cell monolayer 1.5 cm apart. At confluence, the M1 was switched to a second medium (M2), consisting of DMEM with 7% horse serum (Gibco), 0.13 mg/mL of asc-2-phos, 0.05 mg/mL of L-proline, and 2 ng/mL of transforming growth factor beta (TGF- $\beta$ ; Peprotech). Ten of the 30 plates also contained 6 ng/mL of bFGF and  $10^{-8}$  M dex and received the TGF- $\beta$  at confluence (Bone Group 1), another 10 plates were also supplied the bFGF, dex, and TGF- $\beta$ , but the TGF- $\beta$  was administered 5 days after confluence (Bone Group 2). The remaining 10 plates received TGF- $\beta$  at confluence but did not receive bFGF or dex (Bone Group 3). Table 1 lists the medium formulations used in this study. There were no differences in the ability of the cells in each population to form bone-like constructs, and the resulting constructs had similar histological structure and mechanical properties,<sup>19</sup> therefore, results were combined from the three sets. Seven days after construct formation, the diameter of the samples was measured using a reticule in the eyepiece of a Nikon SMZ1500 dissection microscope (Melville, NY).

### *Histochemical and immunofluorescence staining*

Seven days after 3D construct formation, the engineered bone-like constructs (EBCs) were mounted on a holder using tissue freezing medium (Triangle Biomedical Sciences,

TABLE 1. THE TIME AT WHICH EACH MEDIUM FORMULATION WAS INITIALLY ADMINISTERED AND THE MEDIA FORMULATIONS FOR THREE DIFFERENT EBC GROUPS

Time Medium	Day 0 (BMSC Plating) M1	Day 2–4 (BMSC Confluence) M2	Day 7–9 (5 days after BMSC Confluence)
Bone 1		DMEM, 7% HS, asc-2-phos, proline, bFGF, dex, TGF- $\beta$	
Bone 2	DMEM, 20% FBS, bFGF, dex, asc-2-phos, proline	DMEM, 7% HS, asc-2-phos, proline, bFGF, dex	DMEM, 7% HS, asc-2-phos, proline, bFGF, dex, TGF- $\beta$
Bone 3		DMEM, 7% HS, asc-2-phos, proline, TGF- $\beta$	

All bone marrow stromal cells (BMSCs) received the same medium (M1) immediately after isolation. EBC construct dishes received different medium (M2) after BMSCs reached confluence. EBCs from the three groups yielded the same histological and mechanical properties; therefore results were combined.<sup>19</sup>

DMEM, Dulbecco's modified Eagle medium; FBS, fetal bovine serum; dex, dexamethasone; HS, horse serum; asc-2-phos, L-ascorbic acid-2-phosphate; bFGF, basic fibroblast growth factor; TGF- $\beta$ , transforming growth factor beta.

Durham, NC) and immersed in  $-80^{\circ}\text{C}$  isopentane. The frozen samples were sliced longitudinally to a thickness of 9  $\mu\text{m}$  to 12  $\mu\text{m}$  using a Microm HM 500 cryostat system (Heidelberg, Germany). The slides were then used for histological staining for light microscopy or immunofluorescent staining. For histochemical staining, tissue sections were fixed with methanol and stained for calcification with Alizarin Red or hematoxylin and eosin to observe tissue structure. The remaining sections were fixed in acetone and stained for ALP activity.

Immunofluorescent staining was performed to detect the presence of collagen I, collagen II, and osteocalcin. Frozen sections were fixed with methanol for 5 min and rinsed three times with DPBS. Sections were then blocked for 30 min with Ham's F-12 containing 5% donkey serum (Jackson Immuno-Research Labs, Inc, West Grove, PA) at  $37^{\circ}\text{C}$ . Sections were then incubated for 2 h with the primary antibodies in Ham's F-12 containing 1% donkey serum. The concentrations of each of the antibodies were as follows: 5  $\mu\text{g}/\text{mL}$  of rabbit anti-rat collagen I (Abcam Inc., Cambridge, MA), 5  $\mu\text{g}/\text{mL}$  of mouse anti-rat collagen II (Calbiochem, Darmstadt, Germany), and 10  $\mu\text{g}/\text{mL}$  of mouse anti-rat osteocalcin (Abcam). Samples were then rinsed three times with Ham's F-12 and blocked again in Ham's F-12 containing 5% donkey serum at  $37^{\circ}\text{C}$  for 10 min. The secondary antibodies (5  $\mu\text{g}/\text{mL}$ ) were then applied to the sections for 1 h as follows: Alexa Fluor 488 donkey anti-rabbit immunoglobulin (Ig)G (Molecular Probes, Eugene, OR) for collagen I, Alexa Fluor 555 donkey anti-mouse IgG (Molecular Probes) for collagen II, and Alexa Fluor 488 donkey anti-mouse IgG (Molecular Probes) for osteocalcin. Positive and negative control stainings were performed using wheat germ agglutinin lectin and primary antibody omission, respectively (not shown). Nuclei were stained with Prolong Gold antifade reagent with 4',6-diamidino-2-phenylindole (DAPI; Invitrogen). A Nikon Eclipse TS100 microscope equipped with an X-Cite 120 Fluorescence Illumination System was used to image the histochemically and immunofluorescently marked sections. Images were captured using a Diagnostic Instruments Spot Insight Color camera (Sterling Heights, MI).

#### Transmission electron microscopy

Samples were fixed for TEM in 2.5% glutaraldehyde (Electron Microscopy Sciences, Hatfield, PA) in 0.1 M of Sorensen's

buffer, pH 7.4, for 24 h at  $4^{\circ}\text{C}$ . Constructs were then thoroughly rinsed with Sorensen's buffer and post-fixed with 1% osmium tetroxide in Sorensen's buffer for 2 h. Samples were then rinsed with double distilled water and stained with 8% uranyl acetate in double distilled water for 1 h. Constructs were dehydrated in a graded series of ethanol, treated with propylene oxide, and embedded in Epon 812. Longitudinal ultra-thin sections, 70 nm thick, were prepared and stained with uranyl acetate and lead citrate. The sections were examined using a Philips CM100 electron microscope (Bothell, WA) at 60 kV. Images were digitally recorded using a Hamamatsu ORCA-HR digital camera system (Hamamatsu City, Japan) operated using AMT software (Advanced Microscopy Techniques Corp., Danvers, MA).

#### Mechanical properties

Tensile tests were performed on EBCs engineered *in vitro* 7 days ( $n=4$ ) or 6 weeks ( $n=3$ ) after 3D construct formation. Tests were performed using a custom tabletop tensiometer designed in our laboratory, attached to a Nikon SMZ1500 dissection microscope. The sample was immersed in a bath of DPBS, and the ends were grasped using clamps. The dimensions of the sample were measured before each test for cross-sectional area calculation using a reticule in the eyepiece of the microscope. Beads 25  $\mu\text{m}$  in diameter (Interactive Medical Technologies, Irvine, CA) were brushed on the surface of the sample as position markers for digital image correlation analysis of tensile strain. Samples were stretched at a strain rate of 0.01/s. Force was measured using a custom force transducer and monitored using LABVIEW software (National Instruments, Austin, TX); the resolution of the force transducer used for testing the EBCs was 1 mN. Images of the sample were captured using a Basler camera (Exton, PA) attached to the Nikon dissection microscope at a frequency of 2.5/s during the test to follow the location of the digital image correlation markers. The bead position from each image was recorded using LABVIEW software (Melville, NY) with a resolution of 5  $\mu\text{m}$ , and length between beads was calculated by subtracting the position of one bead from another. Nominal stress was calculated using the following equation:

$$\sigma = \frac{F}{A_0}$$

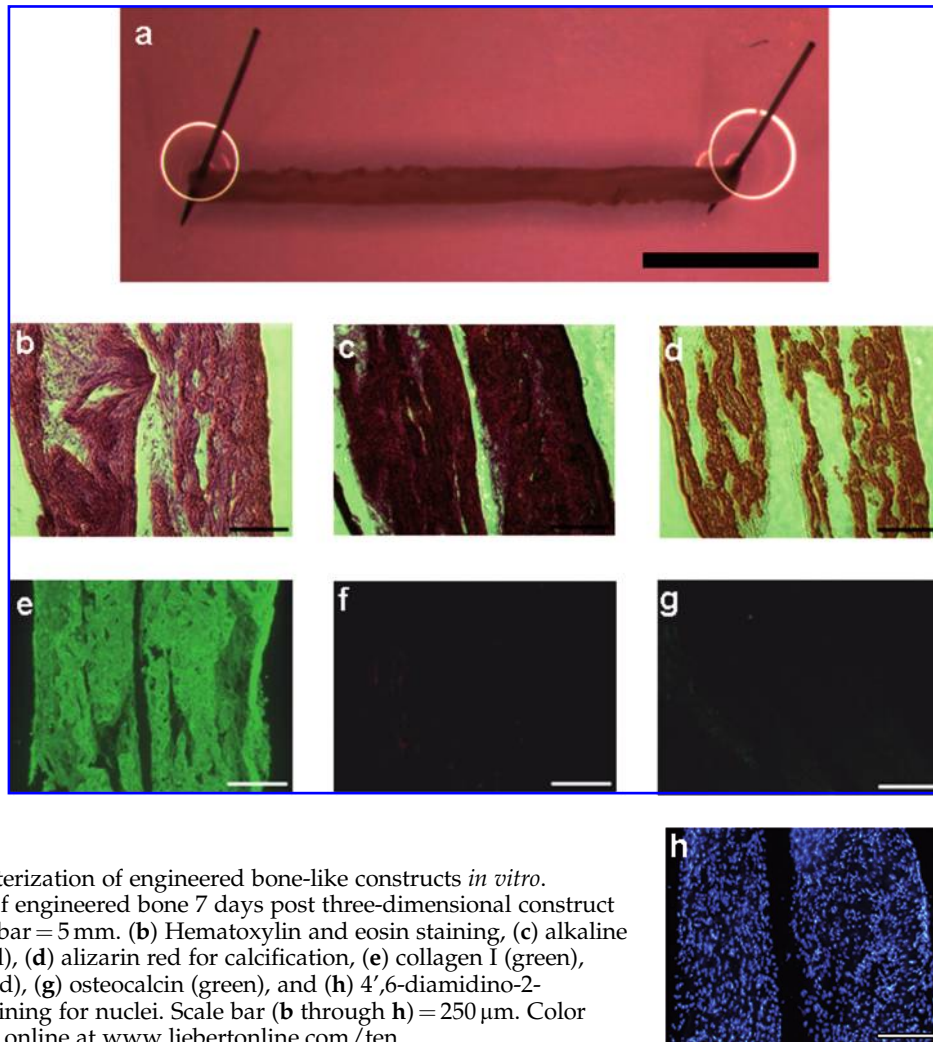


**FIG. 1.** Characterization of engineered bone-like constructs *in vitro*. (a) Photograph of engineered bone 7 days post three-dimensional construct formation, scale bar = 5 mm. (b) Hematoxylin and eosin staining, (c) alkaline phosphatase (red), (d) alizarin red for calcification, (e) collagen I (green), (f) collagen II (red), (g) osteocalcin (green), and (h) 4',6-diamidino-2-phenylindole staining for nuclei. Scale bar (b through h) = 250  $\mu\text{m}$ . Color images available online at [www.liebertonline.com/ten](http://www.liebertonline.com/ten).

Where  $\sigma$  is nominal stress,  $F$  is force, and  $A_0$  is the initial cross-sectional area of the sample. Nominal strain was calculated using the following equation:

$$\varepsilon = \frac{l - l_0}{l_0}$$

Where  $\varepsilon$  is the nominal strain,  $l$  is the current length between beads, and  $l_0$  is the original length. Moduli were obtained by calculating the slope of the tangent of stress versus strain plots at the maximum strain before failure.

### Implantation

Seven days after 3D construct formation, EBCs were placed into a piece of sterile TYGON silicone tubing (United States Plastics Corp., Lima, OH) that had an inner diameter of 1.6 mm, an outer diameter of 3.2 mm, and a length of 1.5 cm. Fisher 344 rats were anesthetized using 0.001 mL of Nembutal sodium solution (pentobarbital sodium injection; Ovation Pharmaceutical Inc., Deerfield, IL) per gram of the animal's weight. The silicone tubes containing the constructs were then implanted between the biceps femoris and the quadriceps of the left leg of the host animals. The silicone

tubing was used to identify the engineered tissue during explantation.

Four weeks after implantation, constructs were removed from the animal. The diameter of the explants was measured using electronic calipers. The samples were then frozen and mounted in tissue freezing medium and stored at  $-80^\circ\text{C}$  or fixed in 2.5% glutaraldehyde and mounted in paraffin for histological studies.

### X-ray diffraction

Wide-angle X-ray scattering diffraction was performed on EBC ( $n=2$ ) samples 6 weeks in culture post-3D construct formation. The bone constructs were removed from their medium and allowed to dry. The engineered tissues were placed on a single-crystal silicon substrate and examined using a Bruker (D8 Discover) diffractometer (Madison, WI) using Cu  $K\alpha$  radiation and a source voltage of 40 kV. The samples were investigated over a  $2\theta$  range of  $23^\circ$  to  $55^\circ$  with 20 counts recorded per degree. Scattering resulting from the substrate was subtracted, and resulting peaks were identified using the hydroxyapatite Powder Diffraction File from the Joint Committee on Powder Diffraction Standards (Swarthmore, PA).<sup>20</sup>

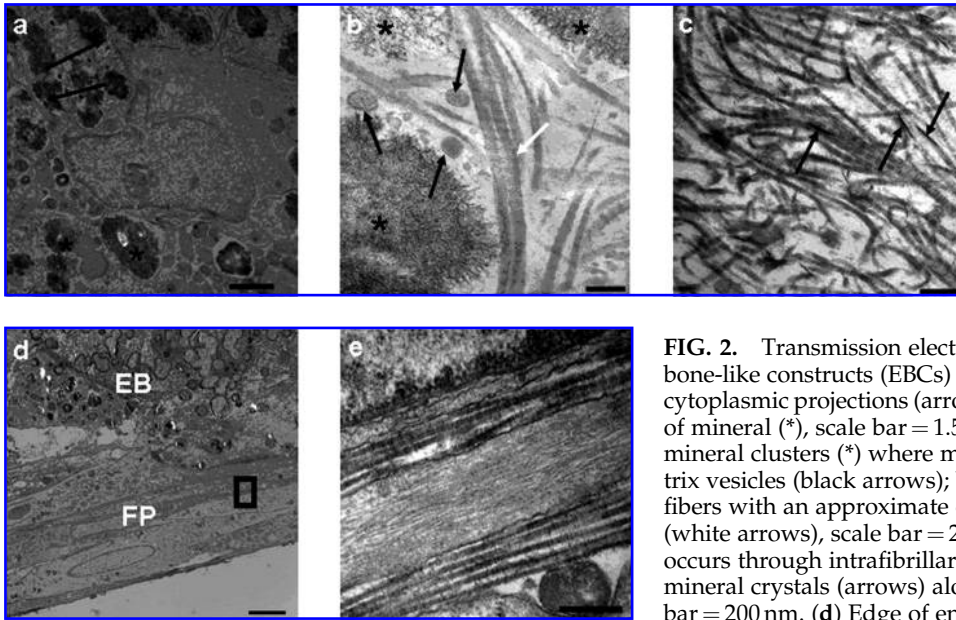


**FIG. 2.** Transmission electron microscopy of engineered bone-like constructs (EBCs) *in vitro*. (a) Osteoblast in EBC has cytoplasmic projections (arrows) and is surrounded by clusters of mineral (\*), scale bar = 1.5  $\mu$ m. (b) Center of tissue shows mineral clusters (\*) where mineralization occurs through matrix vesicles (black arrows); banded collagen I fibers with an approximate diameter of 30 nm are also seen (white arrows), scale bar = 200 nm. (c) Mineralization also occurs through intrafibrillar calcification, as indicated by mineral crystals (arrows) along collagen fibrils, scale bar = 200 nm. (d) Edge of engineered (EB) bone elongated fibroblast-like cells, which may be the onset of periosteum

development, scale bar = 4  $\mu$ m. The boxed area is expanded (e) and shows that the collagen between the fibroblasts in the fibrous periosteum (FP) lacked mineral crystals, scale bar = 300 nm.

## Results

BMSCs were cultured on construct dishes in a medium that induced osteogenic differentiation (M1). Approximately 2 to 4 days after plating, the cells reached confluence and were switched to a second medium (M2) containing a lower serum concentration and TGF- $\beta$ , and two minuten pins were attached to the culture dish as constraint points. After a sufficient amount of ECM was produced, the tissue monolayer lifted from the substrate and contracted radially. The placement of the two constraint points inhibited full contraction, and the monolayer formed into a cylindroid tissue construct of approximately 1.5 cm in length and an elliptical cross-section with major and minor axes of  $1.0 \pm .07$  mm and  $0.78 \pm 0.13$  mm, respectively (Fig. 1a). EBC formation was complete within 14 days of plating the BMSCs onto the cell culture dishes. The resulting engineered tissue was completely solid, which suggests that the cells within the EBCs remodeled the tissue during and after construct formation. The EBCs were kept in culture 7 days or 6 weeks after formation of 3D structure before being fixed for histological and structural characterization.

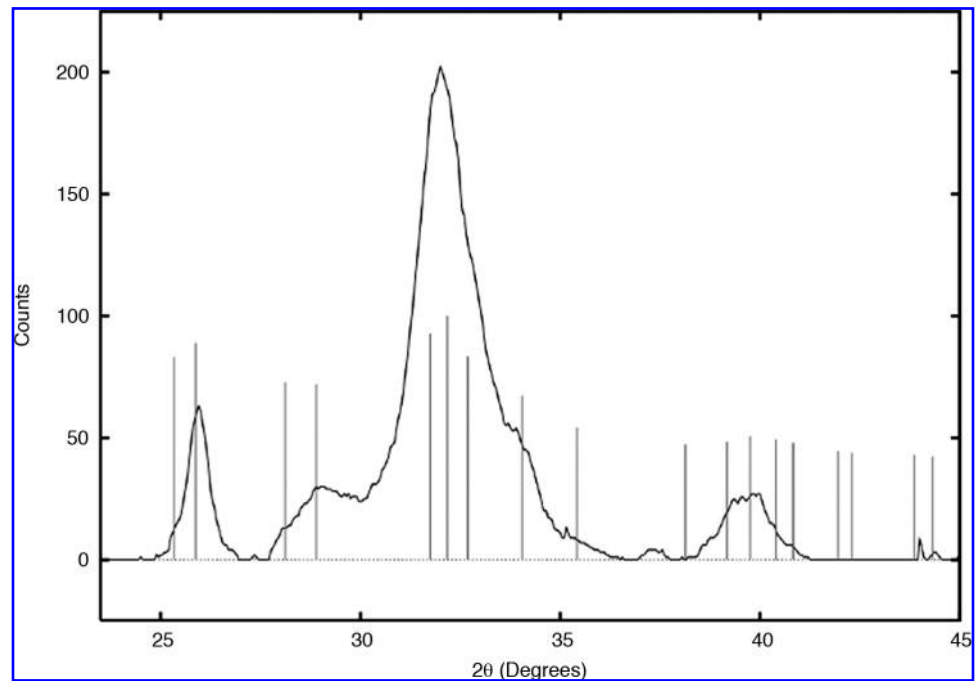
At 7 days post-3D EBC formation, constructs were sectioned longitudinally for histological investigation. Hematoxylin and eosin (H&E) staining revealed that the self-assembled EBCs were composed of dense and fibrous regions (Fig. 1b). The bulk of the tissue stained positive for ALP activity (Fig. 1c), and calcium deposits were located throughout the samples, as seen using Alizarin Red staining (Fig. 1d). The EBCs stained intensely throughout for type I collagen (Fig. 1e) and lacked type II collagen (Fig. 1f), which is consistent with the constitution of native bone. At this point, osteocalcin could not be detected within the EBCs (Fig. 1g). The DAPI-stained cells were fairly uniformly dense throughout the section (Fig. 1h). TEM verified that the EBCs contained osteoblasts (Fig. 2a) in a collagenous matrix un-

dergoing mineralization. The diameter of the collagen was  $29 \pm 4$  nm, which corresponds to the diameter of type I collagen found in the femur.<sup>21</sup> Mineralization was noted to occur through matrix vesicles and intrafibrillar calcification (Fig. 2b, c). Elongated fibroblast-like cells were found on the periphery of the EBCs within axially aligned unmineralized type I collagen (Fig. 2d, e). This structure could be interpreted as the onset of periosteum development. Wide-angle X-ray scattering diffraction peak locations for the EBCs corresponded with those of hydroxyapatite standard (ICDD: 01-073-0293), verifying that the crystals seen in the TEM micrographs were indeed hydroxyapatite (Fig. 3).<sup>20</sup>

The EBCs were able to maintain their size and shape after pins were removed from the edges. When the constructs were lifted and held horizontally at one end with forceps, they did not visibly deflect under their own weight or deform under the pinching loads of the forceps. Unlike (unmineralized) soft tissue constructs that we have engineered in our laboratory that contract longitudinally upon constraint pin removal and cannot support an axial compressive load,<sup>17</sup> the EBCs resist compressive and bending deformation. Tension tests performed on EBCs in culture at 7 days and 6 weeks post-3D EBC formation revealed maximum tangent moduli of  $7.5 \pm 0.5$  MPa ( $n=4$ ) and  $29 \pm 9$  MPa ( $n=3$ ), respectively. The cross-sectional area remained the same between 7 days and 6 weeks post-3D construct formation. The tangent moduli are normalized with respect to the cross-sectional area of the EBCs; therefore, the increase in stiffness between the two time points is a measure of EBC phenotype development and not of physical growth.

At 7 days post-3D construct formation, the EBCs were implanted for 4 weeks between the biceps femoris and quadriceps of Fisher 344 rats. While implanted, the EBCs grew and remodeled so that the resulting explant was cylindrical, with a circular cross-section. The diameter of the explant was  $1.6 \pm 0.3$  mm, equaling the inner diameter of the

**FIG. 3.** Relative intensity (arbitrary units) vs  $2\theta$  (degrees) plot resulting from wide angle X-ray scattering of engineered bone-like constructs. Vertical lines denote the expected peak locations and the relative intensities of the hydroxyapatite standard.<sup>20</sup>



silicone tubing they had been placed in during implantation (Fig. 4a). H&E staining of the demineralized explants revealed a structure that appeared similar to that of native bone (Fig. 4b, c).<sup>22</sup> Osteocytes in lacunae and blood vessels were seen throughout the construct (Fig. 4b, c). Further development of a periosteum-like structure was seen after implantation, as indicated by the fibrous tissue along the edge of the bone explants and the neighboring osteoblast-like cells (Fig. 4b). Alizarin Red staining of explant sections showed greater amounts of calcification (Fig. 4d) than the construct engineered *in vitro* (Fig. 1D). The explanted constructs contained type I collagen and lacked type II (Fig. 4e, f). After implantation, osteocalcin was present within the bone explants (Fig. 4g). DAPI staining (Fig. 4h) showed higher cell densities at regions of lower calcification (Fig. 4d, g vs h). This phenomenon is similar to that in native tissues, in which the cell density is lower in mineralized bone than in surrounding fibrous tissues. TEM of the demineralized explants showed a periosteum-like structure containing osteoprogenitor cells and rows of osteoblast-like cells (Fig 5a). This structure is similar to that of native bone, in which osteoblasts differentiate from progenitor cells within the periosteum in rows and migrate toward the bone matrix.<sup>23</sup> Osteocytes in lacunae were seen within the bone matrix (Fig 5b). Osteoclasts were found throughout the mineralized tissue region (Fig 5c, d). The osteoclasts were identified via their multinucleation (Fig 5c), ruffled borders, and a plethora of vacuoles used by the cell for storage of resorbed material (Fig. 5d).

## Discussion

We have developed a method to engineer 3D bone-like constructs from only BMSCs and their autogenous ECM. After 7 days of post-3D construct formation, the EBCs exhibited ALP activity and contained mineralized type I col-

lagen. The mechanical properties of the EBCs improved over time *in vitro*; tangent stiffness increased by a factor of four over a 5-week period. No significant physical size change occurred *in vitro* from 7 days to 6 weeks in culture after 3D construct formation, indicating phenotype development due to tissue remodeling or increased collagen or mineral production. The phenotype of the EBCs continued to advance during implantation *in vivo*. The explants contained a vascularized bone-like structure with osteoblasts, osteocytes, and osteoclasts. The cell density was in mineralized regions than in the surrounding fibrous areas. The explants contained osteocalcin, which was not detected before implantation, and qualitatively stained more intensely for mineralization. The explants also had a functional periosteum-like tissue containing osteoprogenitor cells that were undergoing differentiation to osteoblasts.

The requirements for bone formation *in vitro* from BMSCs are ascorbic acid, dex, and an organic phosphate.<sup>24</sup> These three components were administered to the BMSCs during the cell proliferation stage of the EBC culture (Table 1). Ascorbic acid maintains connective tissue and regulates ATPase, ALP, and protein synthesis in cultures of osteoblasts. Dex, a synthetic glucocorticoid, stimulates osteoblastic and adipogenic differentiation from BMSCs. Phosphates provide phosphate ions for matrix mineralization.<sup>25,26</sup> In a study published by Maniatopoulos *et al.*, BMSCs were plated on tissue culture plastic to monitor bone formation from BMSCs in two dimensions. The BMSCs were cultured in an osteogenic medium containing ascorbic acid, dex, and an organic phosphate to form bone nodules.<sup>27</sup> Similar to our EBCs, these nodules exhibited ALP activity, were composed of mineralized type I collagen and osteocalcin, and contained osteoblasts and osteocytes. In this previous study, control dishes that lacked dex contained 5 times more cells than dishes that received dex. It is hypothesized that the addition of bFGF to the culture medium allowed for monolayer for-

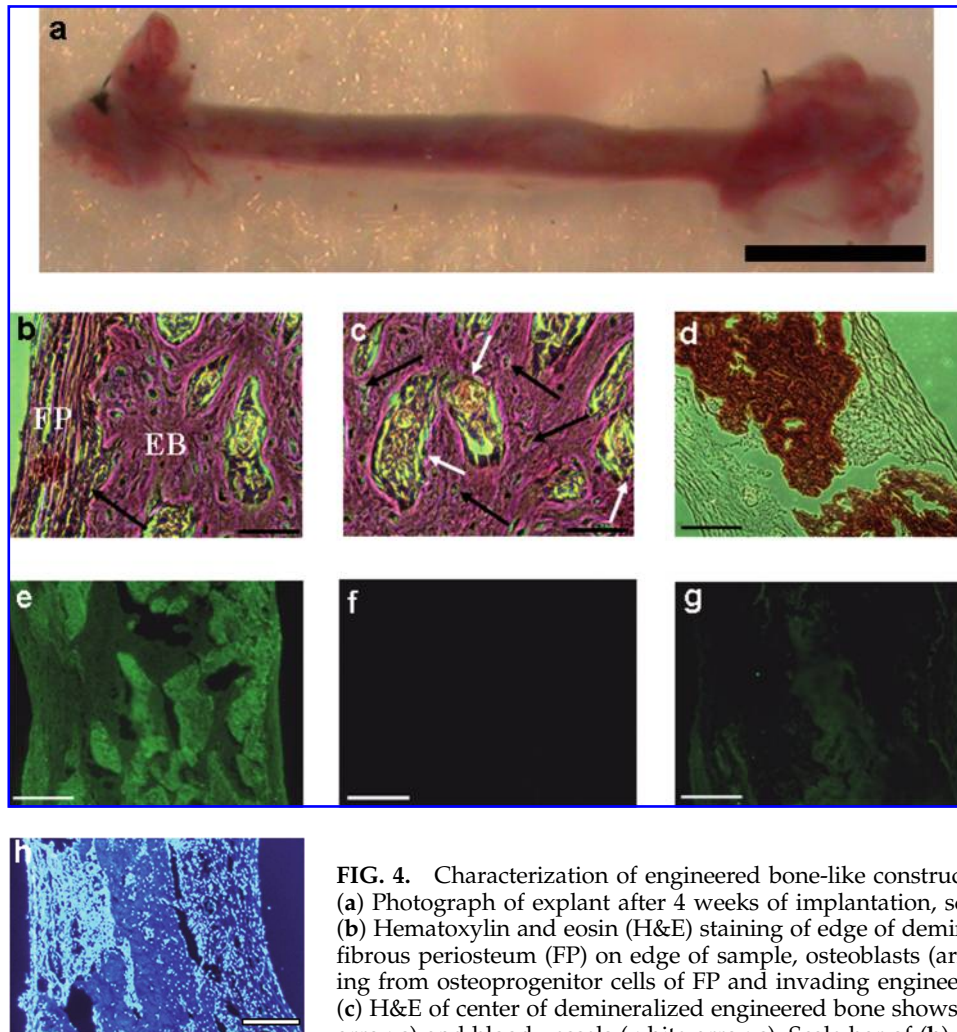


**FIG. 4.** Characterization of engineered bone-like construct (EBC) explants. (a) Photograph of explant after 4 weeks of implantation, scale bar = 5 mm. (b) Hematoxylin and eosin (H&E) staining of edge of demineralized explant, fibrous periosteum (FP) on edge of sample, osteoblasts (arrow) differentiating from osteoprogenitor cells of FP and invading engineered bone (EB). (c) H&E of center of demineralized engineered bone shows osteocytes (black arrows) and blood vessels (white arrows). Scale bar of (b) and (c) = 62.5  $\mu\text{m}$ . (d) Alizarin red staining for calcification, (e) collagen I, (f) collagen II,

(g) osteocalcin, (h) and 4',6-diamidino-2-phenylindole staining for nuclei. Scale bar (d) through (h) = 250  $\mu\text{m}$ . Color images available online at [www.liebertonline.com/ten](http://www.liebertonline.com/ten).

mation rather than the formation of bone nodules. bFGF is commonly used as a potent mitogen for many types of mesenchymal cells. In bone cultures, this cytokine increases mineralization, ALP activity, and the concentrations of bone-specific markers such as calcium and osteocalcin when administered to BMSCs in an osteogenic medium.<sup>27,28</sup> The mitogenic effects of bFGF in addition to dex in the present study may have increased proliferation, thus allowing for monolayer formation rather than the formation of nodules. Control dishes that received M2 lacking TGF- $\beta$  formed cell monolayers that lifted from the substrates but did not contract into cylindrical constructs (data not shown); thus, TGF- $\beta$  is the factor that controls 2D versus 3D construct formation. Although the overall effects of this growth factor on BMSCs are not fully known, it is generally used in culture to stimulate collagen production and matrix maturation and to induce chondrogenic differentiation from BMSCs.<sup>25</sup> In bone cultures, TGF- $\beta$  regulates osteoblast replication and migration, increases ALP activity, and stimulates collagen production and matrix maturation in bone cultures derived from osteogenic cells and BMSCs.<sup>29</sup> We are performing stud-

ies to elucidate the effects of TGF- $\beta$  on 3D bone construct formation with the hypothesis that TGF- $\beta$  increases the rate of collagen production at an early stage of EBC development and before full osteogenic differentiation.

After 4 weeks *in vivo*, the EBCs grew to equal the size of the tubing they was placed into before implantation. It is unknown whether the osteoblasts and osteocytes seen in the EBC explants were derived from the cells present in the EBCs *in vitro* or from precursors from the native blood supply. If some of the osteoblasts and osteocytes developed from the native tissue, this is an indication that the construct provides an optimal scaffold for bone cell infiltration and differentiation even though it was placed in an ectopic site. Explants contained a significant amount of osteocalcin, but this protein was not found in the EBCs before implantation. Osteoclasts were also found within the mineralized matrix of the EBC explants. The observation of osteoprogenitor cells actively differentiating into osteoblasts and the presence of osteoclasts demonstrates that the EBCs actively grew and remodeled *in vivo* in a manner similar to that of native bone.

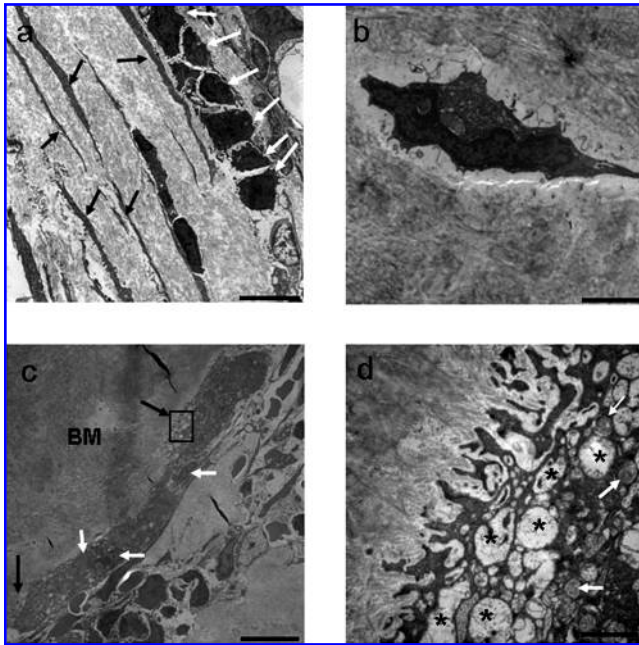


**FIG. 5.** Transmission electron microscopy of engineered bone-like construct explant. (a) Edge of sample has osteoprogenitor cells (black arrows) that are differentiating into osteoblasts (white arrows), indicating periosteum function, scale bar = 8  $\mu\text{m}$ . (b) Osteocyte sitting in lacuna within bone matrix, scale bar = 2  $\mu\text{m}$ . (c) Osteoclast found in engineered bone resorbing demineralized bone matrix (BM) contains several nuclei (white arrows) and ruffled borders (black arrows), distinctions of this cell type, scale bar = 10  $\mu\text{m}$ . Boxed area is magnified (d) to show ruffled border in more detail, notice the empty (\*) and filled (arrows) vacuoles, scale bar = 1  $\mu\text{m}$ .

Before implantation, the periphery of the EBCd contained fibroblast-like cells and unmineralized collagen. This phenomenon is unique to this study and has not yet been reported in 2D bone nodules or in bones engineered with exogenous scaffolding. This structure could be interpreted as the onset of periosteum development. After implantation for 4 weeks, the engineered tissue developed a functional periosteum, as indicated by the presence of osteoprogenitor cells, and rows of osteoblasts (Fig. 5A). If the structure on the periphery of the EBC before implantation was the onset of the periosteum that continued to develop when implanted *in vivo*, it would indicate fibrogenic and osteogenic differentiation from a single cell source *in vitro* within the same culture environment. This could suggest that the BMSCs were differentiating because of the cues delivered through the medium and preferentially as a result of their location within the construct or that the cells differentiated into a mixed population and the fibroblast cells migrated to the outer periphery of the construct upon formation.

The tangent moduli of the EBC at 7 days and 6 weeks in culture post-3D construct formation were  $7.5 \pm 0.5 \text{ MPa}$  and  $29 \pm 9 \text{ MPa}$ , respectively. Previous studies have reported the moduli of unmineralized and mineralized embryonic bone to be 1.11 MPa and 117 MPa, respectively.<sup>30</sup> The mechanical properties of the EBCs are consistent with developing native bone because the moduli lie within the limits of native embryonic bone. The tangent modulus is a measure of constitu-

tive stiffness and is independent of construct size; the increase in EBC tangent moduli between 7 days and 6 weeks in culture post-3D construct formation is therefore an indication of phenotype advancement rather than physical growth.

The method of engineering bone-like structures presented in this study, in which cells are cultured to secrete, assemble, and mineralize their own 3D scaffolding, bypasses the complexity of engineering a scaffold and shifts the paradigm of bone tissue engineering to the guided self-assembly of an autogenous extracellular matrix. Furthermore, this method uses the culture of BMSCs that can be easily isolated from autologous sources without major ethical issues and may be used clinically with minimal risk of rejection. This study is the first to report a functional periosteum-like structure around an engineered bone-like tissue, thus further advancing the state of bone engineering. This novel method of engineering bone-like tissues can be used as a heuristic approach to tissue engineer for large bone defect repair or replacement without the use of an exogenous scaffold and as a model for bone formation through intramembranous ossification. We believe that these scaffold-less bone constructs not only contribute significantly to the field of bone engineering, but also to the field of stem cell research. In this study, osteogenic and fibroblastic differentiation of BMSCs resulted within the same culture environment, suggesting that stem cells may differentiate because of mechanical signals and cues from their location relative to other cells in an engineered construct in addition to chemical signals. Mechanically constraining the contractile monolayer induces tensile strain along the major axis of the constructs and preferentially orients the collagen fibers in this direction. These are the first 3D, scaffold-less tissues developed from bone marrow stem cells that demonstrate phenotype advancement *in vitro* and *in vivo*.

## Acknowledgments

The authors thank Dr. David Martin for his support in wide-angle X-ray diffraction. We would also like to thank Dr. Tatiana Kostrominova and Ms. Kristen Goble for their support in immunofluorescence characterization. This work was partially supported by the National Science Foundation through Award CMS 0200340 and by Defense Advanced Research Projects Agency, through the Biomolecular Motors Program, U.S. Air Force, Office of Scientific Research Award FA9550-05-1-0015.

## References

1. Praemer, A., Furner, S., Rice, D. *Musculoskeletal Conditions in the United States*. Park Ridge, IL: American Academy of Orthopaedic Surgeons, 1992.
2. Salgado, A., Coutinho, O., Reis, R. Bone tissue engineering: state of the art and future trends. *Macromol. Biosci.* **4**, 743, 2004.
3. Ishaug, S.L., Crane G.M., Miller, M.J., Yasko, A.W., Yaszemski, M.J., Mikos, A.G. Bone formation by three-dimensional stromal osteoblast culture in biodegradable polymer scaffolds. *J. Biomed. Mater. Res.* **36**, 17, 1997.
4. Vehof, J. W., Fisher, J.P., Dean, D., van der Waerden, J. C., Spauwen, P.H., Mikos, A.G., Jansen, J.A. Bone formation in transforming growth factor b-1-coated porous poly(propylene fumarate) scaffolds. *J. Biomed. Mater. Res.* **60**, 241, 2002.



5. Peter, S.J., Miller, M.J., Yasko, A.W., Yaszemski, M.J., Mikos, A.G. Polymer concepts in tissue engineering. *J. Biomed. Mater. Res.* **43**, 422, 1998.
6. Ducheyne, P., Qiu, Q. Bioactive ceramics: the effect of surface reactivity on bone formation and bone cell function. *Biomaterials* **20**, 2287, 1999.
7. Zhou, Y., Hutmacher, D., Varawan, S., Lim, T. *In vitro* bone engineering based on polycaprolactone and polycaprolactone-tricalcium phosphate composites. *Polym. Int.* **56**, 333, 2007.
8. Zhou, Y., Chen, F., Ho, S.T., Woodruff, M.A., Lim, T.M., Hutmacher, D.W. Combined marrow stromal cell-sheet techniques and high-strength biodegradable composite scaffolds for engineered functional bone grafts. *Biomaterials* **28**, 814, 2007.
9. Alhadlaq, A., Mao, J. Mesenchymal stem cells: isolation and therapeutics. *Stem Cells Dev.* **13**, 436, 2004.
10. Dezawa, M., Ishikawa, H., Itokazu, Y., Yoshihara, T., Hoshino, M., Takeda, S., Ide, C., Nabeshima, Y. Bone marrow stromal cells generate muscle cells and repair muscle degradation. *Science* **309**, 314, 2005.
11. Pittenger, M.F., Mackay, A.M., Beck, S.C., Jaiswal, R.K., Douglas, R., Mosca, J.D., Moorman, M.A., Simonetti, D.W., Craig, S., Marshak, D.R. Multilineage potential of adult human mesenchymal stem cells. *Science* **284**, 143, 1999.
12. Moreau, J.E., Chen, J., Bramono, D.S., Volloch, V., Chernoff, H., Vunjak-Novakovic, G., Richmond, J.C., Kaplan, D.L., Altman, G.H. Growth factor induced fibroblast differentiation from human bone marrow stromal cells *in vitro*. *J. Orthop. Res.* **23**, 164, 2005.
13. Nauman, E.A., Sakata, T., Keaveny, T.M., Halloran, B.P., Bikle, D.D. bFGF administration lowers the phosphate threshold for mineralization in bone marrow stromal cells. *Calcif. Tissue Int.* **73**, 147, 2003.
14. Marks, S.C., Popoff, S.N. Bone cell biology: the regulation of development, structure, and function in the skeleton. *Am. J. Anat.* **183**, 1, 1988.
15. Taylor, J.F. The periosteum and bone growth. In: Hall, B.K., ed. *Bone*, Vol. 6: Bone Growth-A. Boca Raton, FL: CRC Press Inc., 21, 2000.
16. Dennis, R., Kosnik, P. Excitability and isometric contractile properties of mammalian skeletal muscle constructs engineered *in vitro*. *In Vitro Cell. Dev. Biol. Anim.* **36**, 327, 2000.
17. Calve, S., Dennis, R.G., Kosnik, P.E., Baar, K., Grosh, K., Arruda, E.M. Engineering of functional tendon. *Tissue Eng.* **10**, 755, 2004.
18. Larkin, L., Calve, S.C., Kostrominova, T.Y., and Arruda, E.M. Structure and functional evaluation of tendon-skeletal muscle constructs engineered *in vitro*. *Tissue Eng.* **12**, 3149, 2006.
19. Syed-Picard, F.N. Development and characterization of three dimensional, scaffold-less bone and ligament tissues engineered from bone marrow stem cells [M.S. Thesis]. Department of Materials Science and Engineering, University of Michigan, Ann Arbor, MI, 2006.
20. ICDD Powder Diffraction File. W.F. McClune, ed. International Centre for Diffraction Data, Newtown Square, PA, 2006.
21. Ameye, L., Young, M.F. Mice deficient in small leucine-rich proteoglycans: novel *in vivo* models for osteoporosis osteoarthritic, Ehlers-Danlos syndrome, muscular dystrophy, and corneal diseases. *Glycobiology* **12**, 107R, 2002.
22. Ross, M.H., Romrell, L.J., Kaye, G.I. *Histology: A Text and Atlas*, 3rd Ed. Baltimore, MD: Williams and Wilkins, 1995.
23. Rhodin, J.A.G. *Histology: A Text and Atlas*. London, England: Oxford University Press, 1974.
24. Maniopoulos, C., Sodek, J., Melcher, A.H. Bone formation *in vitro* by stromal cells obtained from bone marrow of young adult rats. *Cell Tissue Res.* **254**, 317, 1988.
25. Locklin, R.M., Oreffo, R., Triffitt, J.T. Effects of TGF- $\beta$  and bFGF on the differentiation of human bone marrow stromal fibroblasts. *Cell Biol. Int.* **23**, 185, 1999.
26. Tenenbaum, H.C. Role of organic phosphate in mineralization of bone *in vitro*. *J. Dent. Res.* **60**, 1586, 1981.
27. Scutt, A., Bertram, P. Basic fibroblast growth factor in the presence of dexamethasone stimulates colony formation, expansion, and osteoblastic differentiation by rat bone marrow stromal cells. *Calcif. Tissue Int.* **64**, 69, 1999.
28. Lisignoli, G., Zini, N., Remiddi, G., Piacentini, A., Puggioli, A., Trimarchi, C., Fini, M., Maraldi, N.M., Facchini, A. Basic fibroblast growth factor enhances *in vitro* mineralization of rat bone marrow stromal cells grown on non-woven hyaluronic acid based polymer scaffold. *Biomaterials.* **22**, 2095, 2001.
29. Johnstone, B., Hering, T.M., Caplan, A.I., Goldberg, V.M., Yoo, J.U. *In vitro* chondrogenesis of bone marrow-derived mesenchymal progenitor cells. *Exp. Cell Res.* **238**, 265, 1998.
30. Tanck, E., Van Donkelaar, C.C., Jepsen, K.J., Goldstein, S.A., Weinans, H., Burger E.H., Huiskes, R. The mechanical consequences of mineralization in embryonic bone. *Bone* **35**, 186, 2004.

Address reprint requests to:

Ellen M. Arruda, Ph.D.  
 Mechanical Engineering  
 Macromolecular Science and Engineering  
 University of Michigan  
 3126 GG Brown  
 Ann Arbor, MI 48109

E-mail: arruda@umich.edu

Received: May 15, 2007

Accepted: May 8, 2008

Online Publication Date: August 29, 2008



**This article has been cited by:**

1. Richard A. Thibault , L. Scott Baggett , Antonios G. Mikos , F. Kurtis Kasper . 2010. Osteogenic Differentiation of Mesenchymal Stem Cells on Pregenerated Extracellular Matrix Scaffolds in the Absence of Osteogenic Cell Culture Supplements. *Tissue Engineering Part A* **16**:2, 431-440. [[Abstract](#)] [[Full Text](#)] [[PDF](#)] [[PDF Plus](#)]
2. Michael J. Smietana, Fatima N. Syed-Picard, Jinjin Ma, Tatiana Kostrominova, Ellen M. Arruda, Lisa M. Larkin. 2009. The effect of implantation on scaffoldless three-dimensional engineered bone constructs. *In Vitro Cellular & Developmental Biology - Animal* **45**:9, 512-522. [[CrossRef](#)]
3. Courtney R. Reed, Li Han, Anthony Andrady, Montserrat Caballero, Megan C. Jack, James B. Collins, Salim C. Saba, Elizabeth G. Lobo, Bruce A. Cairns, John A. van Aalst. 2009. Composite Tissue Engineering on Polycaprolactone Nanofiber Scaffolds. *Annals of Plastic Surgery* **62**:5, 505-512. [[CrossRef](#)]
4. Dongyang Ma, Liling Ren, Yanpu Liu, Fulin Chen, Junrui Zhang, Zhenxun Xue, Tianqiu Mao. 2009. Engineering scaffold-free bone tissue using bone marrow stromal cell sheets. *Journal of Orthopaedic Research* n/a-n/a. [[CrossRef](#)]
5. Jinjin Ma, Kristen Goble, Michael Smietana, Tatiana Kostrominova, Lisa Larkin, Ellen M. Arruda. 2009. Morphological and Functional Characteristics of Three-Dimensional Engineered Bone-Ligament-Bone Constructs Following Implantation. *Journal of Biomechanical Engineering* **131**:10, 101017. [[CrossRef](#)]